Editors' Suggestion

Sampling Efficiency of Transverse Forces in Dense Liquids

Federico Ghimenti,[1] Ludovic Berthier,[2,3] Grzegorz Szamel,[4] and Frédéric van Wijland[1]
[1]Laboratoire Matière et Systèmes Complexes (MSC), Université Paris Cité et CNRS (UMR 7057), 75013 Paris, France
[2]Laboratoire Charles Coulomb (L2C), Université de Montpellier et CNRS (UMR 5221), 34095 Montpellier, France
[3]Yusuf Hamied Department of Chemistry, University of Cambridge, Lensfield Road, Cambridge CB2 1EW, United Kingdom
[4]Department of Chemistry, Colorado State University, Fort Collins, Colorado 80523, USA

(Received 21 July 2023; accepted 22 November 2023; published 18 December 2023)

Sampling the Boltzmann distribution using forces that violate detailed balance can be faster than with the equilibrium evolution, but the acceleration depends on the nature of the nonequilibrium drive and the physical situation. Here, we study the efficiency of forces transverse to energy gradients in dense liquids through a combination of techniques: Brownian dynamics simulations, exact infinite-dimensional calculation, and a mode-coupling approximation. We find that the sampling speedup varies nonmonotonically with temperature, and decreases as the system becomes more glassy. We characterize the interplay between the distance to equilibrium and the efficiency of transverse forces by means of odd transport coefficients.

DOI: 10.1103/PhysRevLett.131.257101

To sample a given target distribution, the paradigm is to construct Markov processes endowed with detailed balance. When the physics slows the dynamics down, as for instance in the vicinity of a critical point, or in disordered and dense systems, algorithms that can increase the sampling efficiency are much needed [1,2]. Sampling by violating detailed balance using nonequilibrium dynamics is a possible route, explored in an applied mathematics literature dating back to the midnineties [3–6]. Potential applications are not limited to physical systems, since, for instance, slow dynamics caused by a complex nonconvex energy landscape are also encountered in machine learning and neural networks [7–10]. Bounds and inequalities on the convergence or mixing rates have been obtained [11–18], and studies encompass the mean-field Ising model [19] and systems evolving via diffusive hydrodynamics [20–22]. This is a very active field of applied mathematics [23,24] and of computer science [25–28]. Numerical studies also exist for a variety of systems [29–37], but no quantitative results exist for systems with self-induced disorder, such as glassy liquids. In the latter case, nonequilibrium forces can either shift [38] or destroy [39] the glass transition, while the addition of unphysical degrees of freedom was recently shown [40] to drastically change the relaxation dynamics.

We explore how nonequilibrium methods that sample the Boltzmann distribution fare when applied to a strongly interacting classical many-body system, such as a high-density or low-temperature fluid exhibiting glassy dynamics, and determine the dependence of the acceleration on the state point. The specific dynamics we study is the overdamped Langevin dynamics driven out of equilibrium by a force field transverse to the local energy gradient. Our results are established using a combination of techniques, ranging from the numerical integration of Langevin equations for a Kob-Andersen mixture, through a mean-field infinite dimensional calculation to finite-dimension mode-coupling approximation. Our presentation goes along these three axes, each of which sheds its own light on the questions we ask.

We demonstrate the existence of an optimal temperature for the acceleration. While a gain remains, the efficiency decreases as the glass transition is approached. Transverse forces also lead to the appearance of odd transport coefficients, that were earlier found in active matter systems composed of chiral particles or driven by nonreciprocal forces [41–43] (see also [44,45] for a dilute equilibrium fluid). Surprisingly, odd diffusivity is insensitive to the emergence of glassy behavior.

Our approach is illustrated with the example of a single particle with position $\mathbf{r}$ in an external potential $V(\mathbf{r})$ at temperature $T = \beta^{-1}$,

$$\frac{d\mathbf{r}}{dt} = -\mu(\mathbf{1} + \gamma\mathbf{A})\partial_{\mathbf{r}}V + \sqrt{2\mu T}\boldsymbol{\eta}, \tag{1}$$

where μ is the mobility. The components of the Gaussian white noise $\boldsymbol{\eta}$ are independent, $\langle \eta_i(t)\eta_j(t')\rangle = \delta_{ij}\delta(t-t')$. When the matrix $\mathbf{A}$ is skew symmetric, the nonequilibrium force of strength γ is transverse to the energy gradient. The stationary distribution thus retains its Boltzmann form, $\rho_{\mathrm{B}}(\mathbf{r}) = \mathrm{e}^{-\beta V(\mathbf{r})}/Z$ even when $\gamma > 0$, but the entropy production rate is finite, $\tau_{\Sigma}^{-1} = \beta\gamma^2\langle(\mathbf{A}\partial_{\mathbf{r}}V)^2\rangle_{\mathrm{B}}$. Another relevant timescale governing microscopic dynamics is given by the reciprocal of the average escape rate [46–48]. Its equilibrium expression is $\tau_0^{-1} \sim \langle\beta(\partial_{\mathbf{r}}V)^2\rangle_{\mathrm{B}}$ but with a nonzero γ this becomes $[\tau_0/(1+\gamma^2\|A\|_{\mathrm{F}}^2/d)]$ (see the

Supplemental Material [49]). This elementary reasoning would suggest that transverse forces simply result in a global rescaling of timescales. We show below that many-body interactions lead to a very different picture.

To widen the scope of our statements, we highlight a correspondence between transverse forces, as defined in Eq. (1), and the lifting procedure [4–6,23,24], which is an alternative approach to accelerate the dynamics. In a nutshell, lifting amounts to augmenting the degrees of freedom of a system with equilibrium dynamics by a set of auxiliary (and unphysical) variables that produce non-equilibrium flows while preserving the original equilibrium distribution. One way to see the connection with transverse forces is to consider, following [33], two equilibrium systems with potentials $V_1(\mathbf{r}_1)$ and $V_2(\mathbf{r}_2)$ evolving through the coupled dynamics

$$\frac{d\mathbf{r}_1}{dt} = \mu(-\partial_{\mathbf{r}_1} V_1 + \gamma \partial_{\mathbf{r}_2} V_2) + \sqrt{2T\mu}\,\boldsymbol{\eta}_1,$$
$$\frac{d\mathbf{r}_2}{dt} = \mu(-\partial_{\mathbf{r}_2} V_2 - \gamma \partial_{\mathbf{r}_1} V_1) + \sqrt{2T\mu}\,\boldsymbol{\eta}_2. \qquad (2)$$

In this case, the nonequilibrium forces are transverse in the extended $(\mathbf{r}_1, \mathbf{r}_2)$ space, and the stationary distribution decouples into $\rho_{\mathrm{B}}(\mathbf{r}_1, \mathbf{r}_2) \propto \mathrm{e}^{-\beta V_1(\mathbf{r}_1)} \mathrm{e}^{-\beta V_2(\mathbf{r}_2)}$. If we choose for system 2 a quadratic potential, the equation of motion for 1 resembles that of an active Ornstein-Uhlenbeck particle [50] where the role of the self-propulsion velocity is played by $\mathbf{r}_2$ [49]. The equation of motion for 2 is however different from the Ornstein-Uhlenbeck equation to ensure that 1 samples the Boltzmann distribution: the dynamics of system 1 is lifted by that of system 2. A cartoon of the connection between transverse forces and lifting is shown in Fig. 1. While our derivations start from transverse forces, our conclusions may therefore extend to some locally lifted systems.

The general many-body problem considered is a system with $i = 1, \ldots, N$ particles in d dimensions evolving under the influence of interparticle forces $\mathbf{F}_i = -(\mathbf{1} + \gamma \mathbf{A}) \sum_{j \neq i} \partial_{\mathbf{r}_i} V(\mathbf{r}_i - \mathbf{r}_j)$, where $\mathbf{A}$ is a skew-symmetric matrix, and $V(\mathbf{r})$ is a pair potential, evolving as in Eq. (1) with thermal noise. The strength of the nonequilibrium forces is controlled by γ which means we keep the matrix elements of $\mathbf{A}$ or order 1 (and independent of γ). The steady state distribution is again the Boltzmann distribution $\rho_{\mathrm{B}} \propto \mathrm{e}^{-\beta \sum_{i<j} V(\mathbf{r}_i - \mathbf{r}_j)}$. We first report the results of numerical simulations of a three-dimensional binary Kob-Andersen mixture [51–53] of $N_A = 800$ particles of type A and $N_B = 200$ of type B interacting as

$$V_{\alpha\beta}(r) = 4\varepsilon_{\alpha\beta}\left[\left(\frac{\sigma_{\alpha\beta}}{r}\right)^{12} - \left(\frac{\sigma_{\alpha\beta}}{r}\right)^{6}\right], \qquad r \leq 2.5\sigma_{\alpha\beta} \quad (3)$$

with $\alpha, \beta \in \{A, B\}$ and where $\varepsilon_{AA} = 1$, $\varepsilon_{AB} = 1.5$, $\varepsilon_{BB} = 0.5$, $\sigma_{AA} = 1$, $\sigma_{AB} = 0.8$, $\sigma_{BB} = 0.88$. The linear size of the system is $9.4\sigma_{AA}$, and periodic boundary conditions were used. We choose $\mathbf{A}$ in a block diagonal form with ± 1 elements in the xy plane, without loss of generality. We integrate the equations of motion using a Euler-Heun algorithm with a discretization step calibrated to optimize efficiency while still properly sampling equilibrium properties [54]. We first show in Fig. 2(a) that the static structure is unaffected by the introduction of transverse forces, demonstrating equilibrium sampling with nonequilibrium dynamics, over a temperature range encompassing a high-temperature almost structureless fluid down to a mildly supercoooled liquid. To estimate the speedup of the sampling, we use the mean-squared displacement $\Delta r^2(t)$ for particles A. Its temperature evolution is shown in Fig. 2(b) at equilibrium, which displays the development of a two-step glassy dynamics below the onset temperature near $T \approx 1.0$.

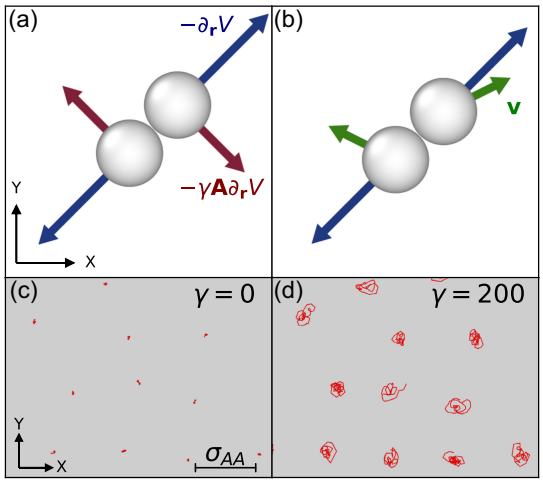

FIG. 1. (a) The addition of transverse forces (red) to the potential ones (blue) acts similarly to (b) a dynamics lifted by additional degrees of freedom (green), by creating an effective chirality. (c) Rendering of a short trajectory for a few particles without any transverse force at $T = 0.8$. (d) Same with transverse forces which induce circular trajectories.

In Fig. 2(c), we demonstrate that the introduction of transverse forces accelerates the dynamics of the system. To quantify this acceleration, we extract the diffusion constant, $D(\gamma, T)$, from the long-time limit of the mean-squared displacements; see Fig. 3(a). At fixed γ, there exists a temperature near $T^* \approx 100$ that maximizes the increase of the diffusion constant.

At high temperatures, interactions (including chiral ones) are smeared out by thermal noise which degrades the efficiency. The initial increase of the acceleration is then well captured by a weak fluctuation expansion [55]. The drop of acceleration as the temperature is lowered can be rationalized by the fact that the energy landscape remains unaffected by the transverse forces. When the supercooled regime is entered more deeply, particles spin along circular trajectories within their local cages; see Figs. 1(c) and 1(d).

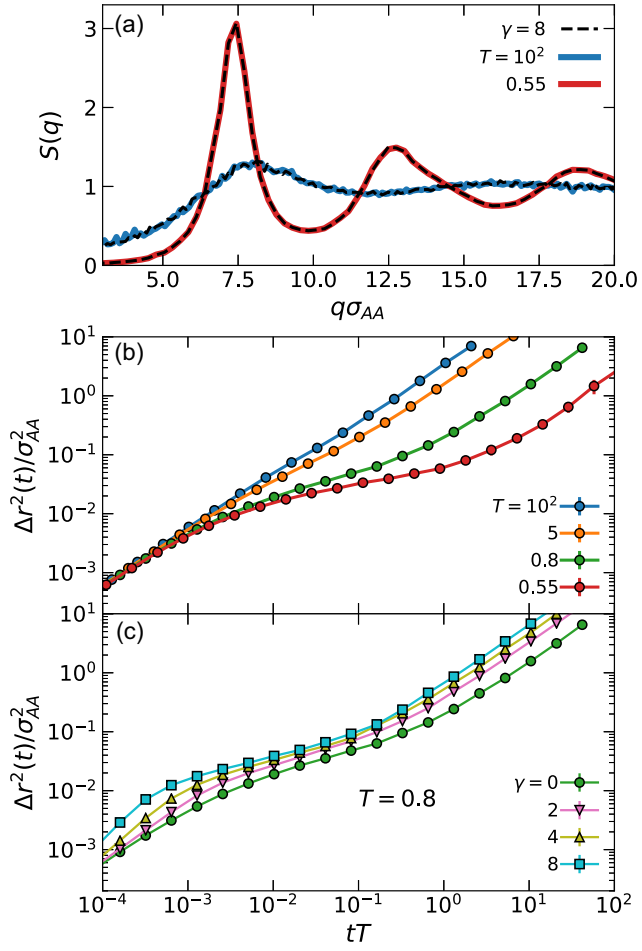

FIG. 2. (a) Static structure factor at $\gamma = 0$ (full color) and $\gamma = 8$ (dashed) at two temperatures. (b) Mean-squared displacement of the A particles for different temperatures. Two-step dynamics becomes visible below the onset temperature near $T\approx = 1.0$. (c) Mean-squared displacement of the A particles at $T = 0.8$ for various values of γ.

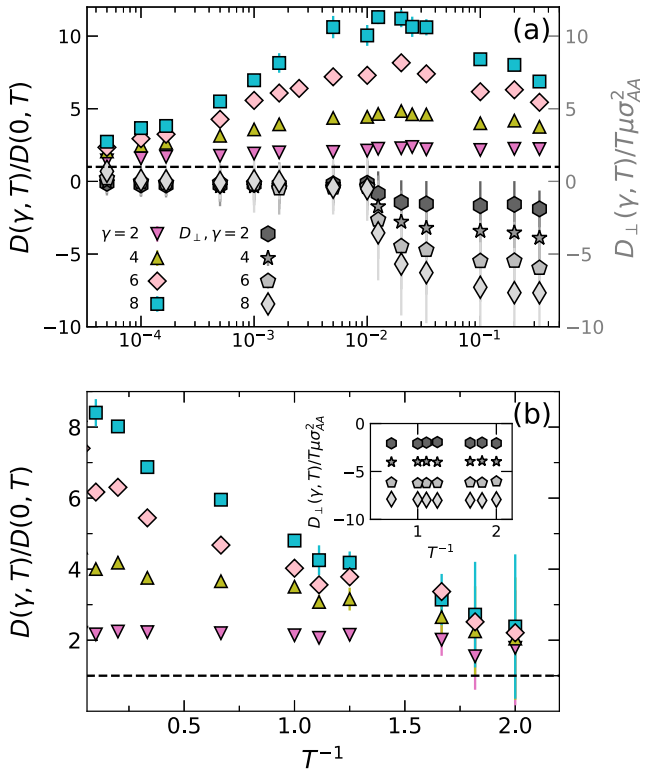

FIG. 3. (a) Diffusion constant $D(\gamma, T)$ normalized by its equilibrium value at $\gamma = 0$ as a function of inverse temperature. The temperature axis uses a logscale to emphasize the nonmonotonic dependence. The right axis describes the odd diffusivity as a function of T^{-1} for various values of γ. (b) Same as (a) using a linear scale to concentrate on the glassy regime below $T = 1.0$. The black dashed line corresponds to the equilibrium efficiency.

This local motion has a modest influence on the long-time dynamics. We thus expect that the glass transition occurs at the same temperature as in equilibrium. These two opposite trends account for the existence of an acceleration maximum.

To confirm the picture of a swirling motion inside a local cage we measure the odd diffusivity of the particles A, which can be calculated from a Green-Kubo expression [41],

$$D_\perp = \frac{1}{2N_A}\sum_{i=1}^{N_A}\int_0^{+\infty} dt\langle \dot{y}_i(t)\dot{x}_i(0) - \dot{x}_i(t)\dot{y}_i(0)\rangle. \quad (4)$$

By symmetry, $D_\perp$ vanishes for an equilibrium dynamics, and its value usefully quantifies the circular motion shown in Fig. 1(d). For example, in the limiting case of a particle trapped in a harmonic well, we show in the Supplemental Material [49] that $D_\perp = -\mu\gamma T$, with μ the mobility of the particle.

The temperature dependence of $D_\perp$ for our simulated system is shown in Fig. 3(a) for different values of γ. Its absolute value increases with γ. At fixed γ, the odd diffusion starts from 0 at high T: as thermal fluctuations wash out interactions, they also suppress particles' chiral motion, which is induced by transverse forces. The modulus of $D_\perp$ then rises steeply as a function of T^{-1} from 0 to a finite value near T^*. As the system enters its slow dynamical regime, $D_\perp$ settles to a finite value as shown in the inset of Fig. 3(b). Interestingly, the observed behavior in the arrested glass phase, where it is presumably dominated by the in-cage circular motion created by the transverse forces, agrees with the predictions for the harmonic well. This contrasts with the translational diffusion coefficient which changes by orders of magnitude in the supercooled liquid, and vanishes in the glass.

Overall the simulations reveal a nonmonotonic temperature dependence of the sampling efficiency of transverse forces, which decreases when temperature is lowered, accompanied by odd diffusivity which appears insensitive to this evolution. To understand these nontrivial findings,

we turn to two analytical approaches, focusing for simplicity on a monodisperse fluid.

First, we consider the mean-field limit which is achieved, for simple fluids, by increasing the space dimension d to infinity [56–60], while keeping the number of neighbors per space direction of order unity. In this limit, one can derive an effective Langevin equation for the position of a tagged particle with an effective noise that originates from the remaining components and the coordinates of all other particles. We defer technical details to [61]. Even out of equilibrium [62,63], the influence of the bath appears as a sum of a position-independent friction kernel and a noise. The friction kernel and the noise autocorrelation need to be determined self-consistently, in a typical mean-field procedure. For our problem, we find that the position $\mathbf{r}_i$ of tagged particle i evolves according to

$$\frac{d\mathbf{r}_i(t)}{dt} = -\mu\beta \int dt' (\mathbf{1}+\gamma\mathbf{A})\mathbf{M}(t-t')\frac{d\mathbf{r}_i(t')}{dt'} + \mathbf{\Xi}_i(t), \qquad (5)$$

where $\mathbf{M}$ is a $d \times d$ memory kernel to be determined, and $\mathbf{\Xi}_i$ is a zero-average Gaussian noise with correlations

$$\langle \mathbf{\Xi}_i(t) \otimes \mathbf{\Xi}_j(t') \rangle = \delta_{ij} \big[2T\mu \mathbf{1}\delta(t-t') + (\mathbf{1}+\gamma\mathbf{A})\mathbf{M}(t-t')(\mathbf{1}-\gamma\mathbf{A}) \big]. \qquad (6)$$

The memory kernel $\mathbf{M}$ is given by correlations of the pair-potential gradients,

$$\mathbf{M}(t) = \sum_j \langle \boldsymbol{\nabla}_i V(\mathbf{r}_{ij}(t)) \otimes \boldsymbol{\nabla}_i V(\mathbf{r}_{ij}(0)) \rangle, \qquad (7)$$

where $\mathbf{r}_{ij} = \mathbf{r}_i - \mathbf{r}_j$. To determine $\mathbf{M}$ we need to consider the evolution of the relative position $\mathbf{r} = \mathbf{r}_{ij}$, which can be shown [61] to follow

$$\frac{1}{2}\frac{d\mathbf{r}}{dt} = -\mu(\mathbf{1}+\gamma\mathbf{A})\partial_{\mathbf{r}} V - \frac{\mu\beta}{2}\int dt' (\mathbf{1}+\gamma\mathbf{A})\mathbf{M}(t-t')\frac{d\mathbf{r}}{dt'} + \mathbf{\Xi}(t), \qquad (8)$$

where the Gaussian noise $\mathbf{\Xi}$ has correlations $\langle \mathbf{\Xi}(t) \otimes \mathbf{\Xi}(t') \rangle = \mathbf{1}T\mu\delta(t-t') + \frac{1}{2}(\mathbf{1}+\gamma\mathbf{A})\mathbf{M}(t-t')(\mathbf{1}-\gamma\mathbf{A})$. The procedure is to determine the statistics of $\mathbf{r}$ as a functional of $\mathbf{M}$, and then to determine the force statistics in the rhs of Eq. (7) as a functional of $\mathbf{M}$, hence obtaining a self-consistent functional equation for $\mathbf{M}$. In practice, even for equilibrium dynamics, $\mathbf{M}$ can only be determined numerically [64]. To evaluate the diffusion constant we only need the time integral of the kernel which becomes diagonal, $\mathbf{M} = \mathbf{1}M$. The diffusion constant is expressed in terms of its time integral $\hat{M}(\gamma, T) = \int_0^{+\infty} M(t)dt$ as

$$D(\gamma, T) = T\mu \frac{1 + (1+\gamma^2)\beta\hat{M}}{(1+\beta\hat{M})^2 + (\beta\gamma\hat{M})^2}. \qquad (9)$$

This result is obtained in even space dimension for a matrix $\mathbf{A}$ [61] made of $d/2$ identical 2×2 blocks with ± 1 entries (nonidentical blocks would require averaging over the blocks, without affecting our conclusions; working in an odd space dimension would involve a single extra space dimension with negligible effect as $d \gg 1$). In the ergodic phase, one can show that the γ-dependent relaxation time of M scales as $\tau(\gamma) = \hat{M} \propto \gamma^{-1}$ when $\gamma \gg 1$. The diffusion constant $D(\gamma, T)$ therefore behaves as $D \sim \gamma$ for large γ. Note also that when $M(t)$ does not relax to 0 then $\hat{M} = +\infty$, and $D(\gamma, T)$ vanishes. We expect that the constraint of Boltzmann sampling is so strong that transverse forces cannot prevent the emergence of diverging free energy barriers leading to ergodicity breaking, in contrast with active forces [38] or shear flows [39]. This implies that the dynamical transition temperature at nonzero γ is unaffected by the transverse forces [61].

The quantity $\hat{M}$ diverges at a finite temperature while a low-density approximation shows [61] that it increases with $1/T$. It is thus natural to expect that $\hat{M}$ is an increasing function of $1/T$. Under this assumption, and looking at Eq. (9), we see that D becomes a nonmonotonous function of temperature. Since the maximum of D occurs at high temperature where memory is weak, it makes sense to evaluate Eq. (9) using a low-density approximation for $\hat{M}$. It turns out that the equilibrium expression of $\hat{M}$ obtained in [64] still holds at nonzero γ [61], and it produces an evolution of D consistent with Fig. 3(a) as explicitly shown in the Supplemental Material [49].

We also obtain the odd diffusivity, given by

$$D_\perp(\gamma, T) = -\gamma T\mu \frac{\beta\hat{M} + (1+\gamma^2)(\beta\hat{M})^2}{(1+\beta\hat{M})^2 + (\gamma\beta\hat{M})^2}, \qquad (10)$$

and which behaves as $D_\perp \sim \gamma$ at large γ. At very high temperature we have $D_\perp = -\gamma\mu\hat{M} \simeq 0$. We also see that $D_\perp = -\gamma\mu T$ below the dynamical transition temperature, when $\hat{M} \to \infty$, consistently with the harmonic well picture [49]. In the mean-field limit, a genuine glass phase appears at low temperature in which particles are trapped in a local harmonic environment created by their neighbors. In a harmonic well the spectrum of the Fokker-Planck operator only picks up an imaginary part when transverse forces are applied, leaving the real part of the eigenvalues unchanged [49], thereby capturing the emergence of circular orbits within the well. The physical picture is that chiral forces eventually lose their accelerating power by wasting the injected energy into circular trajectories.

It is unclear whether these mean-field results are valid in finite dimensions. We thus resort to an approximate theory in the spirit of the mode-coupling theory of glassy dynamics [65]. To compare with the infinite-dimensional calculation we focus on the self-part of the intermediate scattering function, $F_s(\mathbf{q}, t) = (1/N)\sum_j \langle e^{i\mathbf{q}\cdot[\mathbf{r}_j(t) - \mathbf{r}_j(0)]} \rangle$. The long

wavelength limit of $F_s(\mathbf{q};t)$ is related to the mean-squared displacement, $F_s(\mathbf{q}\to 0,t)=1-(q^2/6)\Delta r^2(t)$, and therefore the long time dynamics of F_s at large wavelength allows us to obtain the diffusion constant.

The standard mode-coupling approximation applies to equilibrium dynamics, though recent inroads [66–69] pave the way for nonequilibrium extensions. The main technical difficulty in our case is the presence of transverse currents, which come in addition to the usual longitudinal ones. Within our own mode-coupling approximation for transverse forces, we obtain the memory kernels $(M_\parallel(\mathbf{q},t), M_\perp(\mathbf{q},t))$ encoding respectively longitudinal and transverse current-current correlations. The evolution of $F_s(\mathbf{q},t)$ is given by [55]

$$\partial_t F_s + T\mu q^2 F_s + \mu\beta(1+\gamma^2) M_\perp * F_s = -\left[\mu\beta(M_\parallel + M_\perp) + \mu^2\beta^2(1+\gamma^2)(M_\perp * M_\parallel)\right] * \partial_t F_s, \tag{11}$$

where $*$ denotes a time convolution. The functional expression of $M_\parallel$ is the same as in equilibrium [70], while

$$M_\perp = T^2\rho_0 \int \frac{d\mathbf{k}}{(2\pi)^3}\left(\frac{\mathbf{A}\mathbf{q}\cdot\mathbf{k}}{|\mathbf{A}\mathbf{q}|}\right)^2 c(k)^2 F_s(\mathbf{q}-\mathbf{k},t) S(\mathbf{k},t),$$

with ρ_0 is the number density, $S(\mathbf{k},t)$ the collective intermediate scattering function, and $\rho_0 c(k) \equiv 1 - 1/S(k)$. The same matrix $\mathbf{A}$ as in our numerics is used. To close Eq. (11) we need an equation of motion for $S(\mathbf{q};t)$. This equation, discussed in detail in [55], also predicts that the location of the mode-coupling transition is not influenced by the transverse currents, thus confirming the infinite-dimensional results.

The zero-frequency mode of the memory kernel $\hat{M}_{\alpha,i} = \lim_{q\to 0}\int_0^{+\infty} M_\alpha(q\mathbf{e}_i,t)dt$ controls the behavior of the diffusion constants,

$$D_{\parallel,x} = T\mu \frac{1+(1+\gamma^2)\beta\hat{M}_{\perp,x}}{(1+\beta\hat{M}_{\parallel,x})(1+\beta\hat{M}_{\perp,x}) + \gamma^2\beta^2\hat{M}_{\parallel,x}\hat{M}_{\perp,x}},$$
$$D_{\parallel,z} = \frac{T\mu}{1+\beta\hat{M}_{\parallel,z}}, \tag{12}$$

with $D_{\parallel,y} = D_{\parallel,x}$. We note two consequences of working in finite dimension: $M_\perp \neq M_\parallel$ and $D_{\parallel,z} \neq D_{\parallel,x}$ [note that replacing both $M_\perp$ and $M_\parallel$ with M in Eq. (12) for $D_{\parallel,x}$ leads back to the infinite-dimensional expression Eq. (9)]. Assuming that the system falls into a nonergodic regime below some transition temperature T_{MCT}, the memory kernels $M_\perp(t)$ and $M_\parallel(t)$ also saturate at a nonzero value at long times, and the longitudinal diffusion constants vanish. Whereas the location of the ergodicity-breaking transition is independent of γ, the dynamics in the ergodic phase is not. In particular, assuming that $\hat{M}_{\parallel,i}$ does not exceed its equilibrium counterpart, one can show that the longitudinal diffusion constants for $\gamma \neq 0$ are always larger than their equilibrium counterpart. If the diffusion constant is larger, the long time relaxation of F_s is faster, and thus the value of the zero-frequency limit of the kernels is reduced, self-consistently demonstrating acceleration of the dynamics for $\gamma > 0$. Remarkably, Eq. (12) shows that the diffusion (quantified by $D_{\parallel,z}$) along the z direction is also indirectly accelerated by the coupling with the other directions. Overall, the mode-coupling calculation highlights interesting differences with the large d limit, but the main results are in agreement.

In conclusion, we found that the acceleration provided by transverse forces in a dense interacting system strongly depends on temperature, which comes as a surprise. The acceleration departs from a simple rescaling of the time, due to both interactions and emerging glassiness, which also lead to nontrivial asymptotic scaling with γ. Transverse forces begin to operate when the relaxation time of the system exceeds $\tau_\Sigma \sim \tau_0/\gamma^2$, but their efficiency decreases in deeply supercooled states leading instead to circular trajectories but only modest acceleration. This picture is corroborated by the behavior of the odd diffusivity, which is small as long as τ_Σ exceeds the relaxation rate of the system, but saturates to a finite value as the glass phase is approached. Our Letter resorts to a very local, and somewhat uninformed, way of driving the system out of equilibrium. In the more elaborate methods implemented in [31,71], spatially extended and correlated moves are performed. It is a stimulating open question to find out how, when pushed toward glassiness, these methods compare with the minimal ones investigated here.

L. B., F. G., and F. vW. acknowledge the financial support of the ANR THEMA AAPG2020 grant, along with several discussions with M. Michel, A. Guillin, and W. Krauth. G. S. acknowledges the support of NSF Grant No. CHE 2154241.

[1] W. Krauth, Event-chain Monte Carlo: Foundations, applications, and prospects, Front. Phys. **9**, 663457 (2021).
[2] L. Berthier and D. R. Reichman, Modern computational studies of the glass transition, Nat. Rev. Phys. **5**, 1 (2023).
[3] C.-R. Hwang, S.-Y. Hwang-Ma, and S.-J. Sheu, Accelerating Gaussian diffusions, Ann. Appl. Probab. **3**, 897 (1993).
[4] F. Chen, L. Lovász, and I. Pak, Lifting Markov chains to speed up mixing, in *Proceedings of the 31st Annual ACM Symposium Theory of Computing* (Association for Computing Machinery, New York, 1999), pp. 275–281.
[5] P. Diaconis, S. Holmes, and R. M. Neal, Analysis of a nonreversible Markov chain sampler, Ann. Appl. Probab. **10**, 726 (2000).
[6] M. Vucelja, Lifting—a nonreversible Markov chain Monte Carlo algorithm, Am. J. Phys. **84**, 958 (2016).

[7] M. Ohzeki, Stochastic gradient method with accelerated stochastic dynamics, J. Phys. Conf. Ser. **699**, 012019 (2016).
[8] X. Gao, M. Gurbuzbalaban, and L. Zhu, Breaking reversibility accelerates Langevin dynamics for non-convex optimization, Adv. Neural Inf. Process. Syst. **33**, 17850 (2020).
[9] F. Futami, I. Sato, and M. Sugiyama, Accelerating the diffusion-based ensemble sampling by non-reversible dynamics, in *International Conference on Machine Learning* (PMLR, Cambridge, 2020), pp. 3337–3347.
[10] F. Futami, T. Iwata, N. Ueda, and I. Sato, Accelerated diffusion-based sampling by the non-reversible dynamics with skew-symmetric matrices, Entropy **23**, 993 (2021).
[11] B. Franke, C.-R. Hwang, H.-M. Pai, and S.-J. Sheu, The behavior of the spectral gap under growing drift, Trans. Am. Math. Soc. **362**, 1325 (2010).
[12] A. Ichiki and M. Ohzeki, Violation of detailed balance accelerates relaxation, Phys. Rev. E **88**, 020101(R) (2013).
[13] T. Lelièvre, F. Nier, and G. A. Pavliotis, Optimal nonreversible linear drift for the convergence to equilibrium of a diffusion, J. Stat. Phys. **152**, 237 (2013).
[14] L. Rey-Bellet and K. Spiliopoulos, Irreversible Langevin samplers and variance reduction: A large deviations approach, Nonlinearity **28**, 2081 (2015).
[15] C.-R. Hwang, R. Normand, and S.-J. Wu, Variance reduction for diffusions, Stoch. Proc. Appl. **125**, 3522 (2015).
[16] A. B. Duncan, T. Lelievre, and G. A. Pavliotis, Variance reduction using nonreversible Langevin samplers, J. Stat. Phys. **163**, 457 (2016).
[17] D. A. Levin and Y. Peres, *Markov Chains and Mixing Times* (American Mathematical Society, Providence, 2017), Vol. 107.
[18] S. Apers, A. Sarlette, and F. Ticozzi, When does memory speed-up mixing?, in *2017 IEEE 56th Annual Conference on Decision and Control (CDC)* (IEEE, Hoboken, 2017), pp. 4940–4945.
[19] C. Monthus, Large deviations for the skew-detailed-balance lifted-Markov processes to sample the equilibrium distribution of the Curie–Weiss model, J. Stat. Mech. (2021) 103202.
[20] M. Kaiser, R. L. Jack, and J. Zimmer, Acceleration of convergence to equilibrium in Markov chains by breaking detailed balance, J. Stat. Phys. **168**, 259 (2017).
[21] M. Kaiser, R. L. Jack, and J. Zimmer, Canonical structure and orthogonality of forces and currents in irreversible Markov chains, J. Stat. Phys. **170**, 1019 (2018).
[22] F. Coghi, R. Chetrite, and H. Touchette, Role of current fluctuations in nonreversible samplers, Phys. Rev. E **103**, 062142 (2021).
[23] S. Chatterjee and P. Diaconis, Correction to: Speeding up Markov chains with deterministic jumps, Probab. Theory Relat. Fields **181**, 377 (2021).
[24] B. Franke, C.-R. Hwang, A. O. Said, and H.-M. Pai, A note on the asymptotic variance of drift accelerated diffusions, Stat. Probab. Lett. **175**, 109128 (2021).
[25] S. Apers, F. Ticozzi, and A. Sarlette, Lifting Markov chains to mix faster: Limits and opportunities, arXiv:1705.08253.
[26] S. Apers, A. Sarlette, and F. Ticozzi, Fast mixing with quantum walks vs. classical processes, in *Quantum Information Processing (QIP) 2017* (2017).
[27] S. Apers, A. Sarlette, and F. Ticozzi, Simulation of quantum walks and fast mixing with classical processes, Phys. Rev. A **98**, 032115 (2018).
[28] S. Apers, A. Sarlette, and F. Ticozzi, Characterizing limits and opportunities in speeding up Markov chain mixing, Stoch. Proc. Appl. **136**, 145 (2021).
[29] E. P. Bernard, W. Krauth, and D. B. Wilson, Event-chain Monte Carlo algorithms for hard-sphere systems, Phys. Rev. E **80**, 056704 (2009).
[30] E. P. Bernard and W. Krauth, Two-step melting in two dimensions: First-order liquid-hexatic transition, Phys. Rev. Lett. **107**, 155704 (2011).
[31] S. C. Kapfer and W. Krauth, Irreversible local Markov chains with rapid convergence toward equilibrium, Phys. Rev. Lett. **119**, 240603 (2017).
[32] M. Isobe and W. Krauth, Hard-sphere melting and crystallization with event-chain Monte Carlo, J. Chem. Phys. **143**, 084509 (2015).
[33] M. Ohzeki and A. Ichiki, Langevin dynamics neglecting detailed balance condition, Phys. Rev. E **92**, 012105 (2015).
[34] M. Michel, J. Mayer, and W. Krauth, Event-chain Monte Carlo for classical continuous spin models, Europhys. Lett. **112**, 20003 (2015).
[35] Y. Sakai and K. Hukushima, Dynamics of one-dimensional Ising model without detailed balance condition, J. Phys. Soc. Jpn. **82**, 064003 (2013).
[36] K. S. Turitsyn, M. Chertkov, and M. Vucelja, Irreversible Monte Carlo algorithms for efficient sampling, Physica (Amsterdam) **240D**, 410 (2011).
[37] F. Ghimenti and F. van Wijland, Accelerating, to some extent, the p-spin dynamics, Phys. Rev. E **105**, 054137 (2022).
[38] L. Berthier and J. Kurchan, Non-equilibrium glass transitions in driven and active matter, Nat. Phys. **9**, 310 (2013).
[39] L. Berthier, J.-L. Barrat, and J. Kurchan, A two-time-scale, two-temperature scenario for nonlinear rheology, Phys. Rev. E **61**, 5464 (2000).
[40] A. Ninarello, L. Berthier, and D. Coslovich, Models and algorithms for the next generation of glass transition studies, Phys. Rev. X **7**, 021039 (2017).
[41] C. Hargus, J. M. Epstein, and K. K. Mandadapu, Odd diffusivity of chiral random motion, Phys. Rev. Lett. **127**, 178001 (2021).
[42] A. R. Poggioli and D. T. Limmer, Odd mobility of a passive tracer in a chiral active fluid, Phys. Rev. Lett. **130**, 158201 (2023).
[43] D. Banerjee, A. Souslov, A. G. Abanov, and V. Vitelli, Odd viscosity in chiral active fluids, Nat. Commun. **8**, 1573 (2017).
[44] E. Kalz, H. D. Vuijk, I. Abdoli, J.-U. Sommer, H. Löwen, and A. Sharma, Collisions enhance self-diffusion in odd-diffusive systems, Phys. Rev. Lett. **129**, 090601 (2022).
[45] E. Kalz, H. D. Vuijk, J.-U. Sommer, R. Metzler, and A. Sharma, Oscillatory force autocorrelations in equilibrium odd-diffusive systems, arXiv:2302.01263.
[46] E. Pitard, V. Lecomte, and F. Van Wijland, Dynamic transition in an atomic glass former: A molecular-dynamics evidence, Europhys. Lett. **96**, 56002 (2011).

[47] C. J. Fullerton and R. L. Jack, Dynamical phase transitions in supercooled liquids: Interpreting measurements of dynamical activity, J. Chem. Phys. **138**, 224506 (2013).
[48] C. Maes, Frenesy: Time-symmetric dynamical activity in nonequilibria, Phys. Rep. **850**, 1 (2020).
[49] See Supplemental Material at http://link.aps.org/supplemental/10.1103/PhysRevLett.131.257101 for contains some technical details for the derivation of our results.
[50] N. Koumakis, C. Maggi, and R. Di Leonardo, Directed transport of active particles over asymmetric energy barriers, Soft Matter **10**, 5695 (2014).
[51] W. Kob and H. C. Andersen, Scaling behavior in the β-relaxation regime of a supercooled Lennard-Jones mixture, Phys. Rev. Lett. **73**, 1376 (1994).
[52] W. Kob and H. C. Andersen, Testing mode-coupling theory for a supercooled binary Lennard-Jones mixture I: The Van Hove correlation function, Phys. Rev. E **51**, 4626 (1995).
[53] E. Flenner and G. Szamel, Relaxation in a glassy binary mixture: Comparison of the mode-coupling theory to a Brownian dynamics simulation, Phys. Rev. E **72**, 031508 (2005).
[54] T. Gleim, W. Kob, and K. Binder, How does the relaxation of a supercooled liquid depend on its microscopic dynamics?, Phys. Rev. Lett. **81**, 4404 (1998).
[55] F. Ghimenti, L. Berthier, G. Szamel, and F. van Wiljand, Transverse forces, a mode-coupling investigation (to be published).
[56] H. L. Frisch, N. Rivier, and D. Wyler, Classical hard-sphere fluid in infinitely many dimensions, Phys. Rev. Lett. **54**, 2061 (1985).
[57] G. Parisi and F. Zamponi, Mean-field theory of hard sphere glasses and jamming, Rev. Mod. Phys. **82**, 789 (2010).
[58] T. Maimbourg, J. Kurchan, and F. Zamponi, Solution of the dynamics of liquids in the large-dimensional limit, Phys. Rev. Lett. **116**, 015902 (2016).
[59] G. Parisi, P. Urbani, and F. Zamponi, *Theory of Simple Glasses* (Cambridge University Press, Cambridge, England, 2020).
[60] C. Liu, G. Biroli, D. R. Reichman, and G. Szamel, Dynamics of liquids in the large-dimensional limit, Phys. Rev. E **104**, 054606 (2021).
[61] F. Ghimenti, L. Berthier, G. Szamel, and F. van Wiljand, Transverse forces in infinite dimensions.
[62] E. Agoritsas, T. Maimbourg, and F. Zamponi, Out-of-equilibrium dynamical equations of infinite-dimensional particle systems. I. the isotropic case, J. Phys. A **52**, 144002 (2019).
[63] E. Agoritsas, T. Maimbourg, and F. Zamponi, Out-of-equilibrium dynamical equations of infinite-dimensional particle systems. II. The anisotropic case under shear strain, J. Phys. A **52**, 334001 (2019).
[64] A. Manacorda, G. Schehr, and F. Zamponi, Numerical solution of the dynamical mean field theory of infinite-dimensional equilibrium liquids, J. Chem. Phys. **152**, 164506 (2020).
[65] W. Götze, *Complex Dynamics of Glass-Forming Liquids* (Oxford University Press on Demand, 2009), Vol. 143.
[66] M. Fuchs and M. E. Cates, A mode coupling theory for Brownian particles in homogeneous steady shear flow, J. Rheol. **53**, 957 (2009).
[67] G. Szamel, Theory for the dynamics of dense systems of athermal self-propelled particles, Phys. Rev. E **93**, 012603 (2016).
[68] A. Liluashvili, J. Ónody, and T. Voigtmann, Mode-coupling theory for active Brownian particles, Phys. Rev. E **96**, 062608 (2017).
[69] G. Szamel, Mode-coupling theory for the steady-state dynamics of active Brownian particles, J. Chem. Phys. **150**, 124901 (2019).
[70] U. Bengtzelius, W. Gotze, and A. Sjolander, Dynamics of supercooled liquids and the glass transition, J. Phys. C **17**, 5915 (1984).
[71] M. Michel, S. C. Kapfer, and W. Krauth, Generalized event-chain Monte Carlo: Constructing rejection-free global-balance algorithms from infinitesimal steps, J. Chem. Phys. **140**, 054116 (2014).